Monthly Notices
of the
ROYAL ASTRONOMICAL SOCIETY

MNRAS **453,** 951–959 (2015) doi:10.1093/mnras/stv1618

A millimetre-wave redshift search for the unlensed HyLIRG, HS1700.850.1

S. C. Chapman,[1⋆] F. Bertoldi,[2] Ian Smail,[3] C. C. Steidel,[4] A. W. Blain,[5] J. E. Geach,[6] M. Gurwell,[7] R. J. Ivison,[8,9] G. R. Petitpas[7] and N. Reddy[10]

[1]*Department of Physics and Atmospheric Science, Dalhousie University, Halifax, NS B3H 4R2, Canada*
[2] *Argelander-Institute of Astronomy, Bonn University, Auf dem Hugel 71, D-53121 Bonn, Germany*
[3]*Centre for Extragalactic Astronomy, Department of Physics, Durham University, South Road, Durham DH1 3LE, UK*
[4]*Cahill Center for Astronomy and Astrophysics, California Institute of Technology, MS 249-17, Pasadena, CA 91125, USA*
[5]*Physics and Astronomy, University of Leicester, University Road Leicester, Leicester LE1 7RH, UK*
[6]*Centre for Astrophysics Research, Science & Technology Research Institute, University of Hertfordshire, Hatfield AL10 9AB, UK*
[7]*Harvard–Smithsonian Center for Astrophysics, 60 Garden Street, Cambridge, MA 02138, USA*
[8]*Institute for Astronomy, University of Edinburgh, Royal Observatory, Blackford Hill, Edinburgh EH9 3HJ, UK*
[9]*European Southern Observatory, Karl Schwarzschild Strasse 2, D-85748 Garching, Germany*
[10]*Department of Physics and Astronomy, UC Riverside, 900 University Avenue, Riverside, CA 92521, USA*

Accepted 2015 July 15. Received 2015 July 14; in original form 2015 March 5

ABSTRACT

We report the redshift of an unlensed, highly obscured submillimetre galaxy (SMG), HS1700.850.1, the brightest SMG ($S_{850\,\mu m} = 19.1$ mJy) detected in the James Clerk Maxwell Telescope/Submillimetre Common-user Bolometer Array-2 (JCMT/SCUBA-2) Baryonic Structure Survey, based on the detection of its ^{12}CO line emission. Using the Institute Radio Astronomie Millimetrique Plateau de Bure Interferometer with 3.6 GHz band width, we serendipitously detect an emission line at 150.6 GHz. From a search over 14.5 GHz in the 3- and 2-mm atmospheric windows, we confirm the identification of this line as ^{12}CO(5–4) at $z = 2.816$, meaning that it does not reside in the $z \sim 2.30$ proto-cluster in this field. Measurement of the 870 μm source size (<0.85 arcsec) from the Sub-Millimetre Array (SMA) confirms a compact emission in a $S_{870\,\mu m} = 14.5$ mJy, $L_{IR} \sim 10^{13}$ L$_\odot$ component, suggesting an Eddington-limited starburst. We use the double-peaked ^{12}CO line profile measurements along with the SMA size constraints to study the gas dynamics of a HyLIRG, estimating the gas and dynamical masses of HS1700.850.1. While HS1700.850.1 is one of the most extreme galaxies known in the Universe, we find that it occupies a relative void in the Lyman-Break Galaxy distribution in this field. Comparison with other extreme objects at similar epochs (HyLIRG Quasars), and cosmological simulations, suggests such an *anti-bias* of bright SMGs could be relatively common, with the brightest SMGs rarely occupying the most overdense regions at $z = 2$–4.

Key words: galaxies: abundances – galaxies: high-redshift – submillimetre: galaxies.

1 INTRODUCTION

Blank-field mm and sub-mm continuum surveys have discovered hundreds of dusty, star-forming sub-mm galaxies (SMGs) over the past decade (e.g. Smail et al. 2002; Borys et al. 2003; Greve et al. 2004; Coppin et al. 2006; Bertoldi et al. 2007; Scott et al. 2008; Weiss et al. 2009), while *Herschel*-SPIRE has mapped close to 10^3 deg^2 in the 500, 350, 250 μm bands, leading to $\sim 10^4$ SMGs being detected (e.g. Oliver et al. 2010). At higher flux limits, SPT has mapped 2500 deg^2 (e.g. Mocanu et al. 2013), and *Planck* has mapped the entire sky (Planck collaboration XXVIII et al. 2014), finding many extreme and/or gravitationally lensed SMGs. The search for the most luminous star-forming galaxies from hundreds of deg^2 in the Universe has ensued (e.g. Fu et al. 2013, Ivison et al. 2013). However, some of the SMGs discovered in early ∼100 arcmin^2 surveys remain the intrinsically brightest, most extreme known (e.g. SMM J02399 – Ivison et al. 1998, 2010, GN20 – Pope et al. 2006; Younger et al. 2008, and COSMOS-AzTEC1 – Scott et al. 2008; Younger et al. 2010).

Determining the redshifts of unlensed SMGs has largely been a process of using weak counterparts in the rest-frame ultraviolet and optical to make spectroscopic determinations (e.g. Chapman et al. 2003, 2005), or combining near- and mid-IR photometry to obtain

⋆ E-mail: scott.chapman@dal.ca

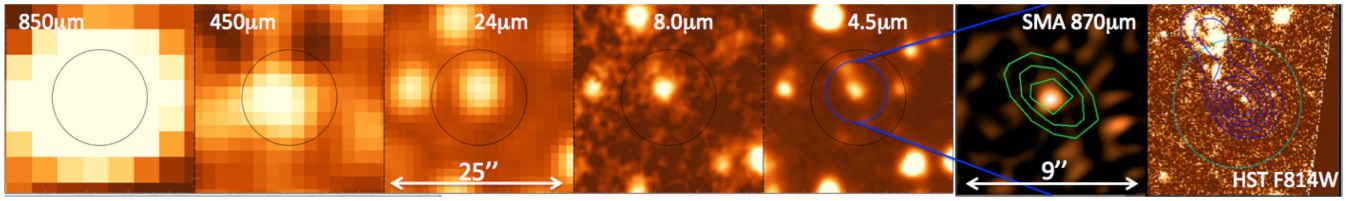

Figure 1. Left to right: five cutout images 25 arcsec on a side of the longer wavelength data for HS1700.850.1 (850 μm, 450 μm, 24 μm, 8 μm, 4.5 μm), highlighting the likely identification of the SMG with an IR-luminous component (black circle shows the 15 arcsec SCUBA-2 beam size). Second from right: A 9 × 9 arcsec^2 zoom in from the SMA compact+extended configuration 870 μm map, with a ∼ 0.74 arcsec synthesized beam with PdBI ^{12}CO(5–4) contours overlaid. Most of the SCUBA-2 flux (14.5 mJy) is recovered in a single compact component, unresolved with a 1 arcsec beamsize. No other significant sources are detected within the 15 arcsec diameter of the SCUBA-2 beam. Further, the compact configuration data on its own measure a flux of 19 ± 3 mJy, comparable to the SCUBA-2 flux, and suggest that the source may be marginally resolved on scales >1 arcsec. Far right: 9 arcsec cutout of the *HST*-ACS F814W image centred on the SMA detection, with IRAC ch-2 contours overlaid, shows HS1700.850.1 to be well identified with a faint tad-pole like $I_{AB} \sim 26$ galaxy, which is marginally detected in ground-based imaging ($\mathcal{R} = 26.1$).

reliable photometric redshift estimates (e.g. Wardlow et al. 2011; Simpson et al. 2014). However, because the high extinction of SMGs means that they often have only very faint (if any) counterparts in the optical/near-IR bands, the spectroscopic and even photometric redshift distributions have remained incomplete and biased (e.g. Simpson et al. 2014).

The largest spectroscopic SMG redshift survey to date was based on radio-identified SMGs (Chapman et al. 2005). The radio identification is sometimes inaccurate (Hodge et al. 2013) and may bias the redshift distribution since radio emission may remain undetected even in the deepest radio maps for sources at $z > 3$. Optical spectroscopic followup to Atacama Large Millimeter Array (ALMA)-identified SMGs (Simpson et al. 2014; Danielson et al., in preparation) has removed the identification bias, but cannot remove the spectroscopic bias.

An alternative route to determine the redshift of an SMG is through observations of ^{12}CO emission lines at cm or mm wavelengths. The ^{12}CO lines arise from the molecular gas, the fuel for star formation, and can thus be related unambiguously to the sub-mm continuum source. Therefore, these observations do not require any additional multi-wavelength identification and circumvent many of the problems inherent to optical spectroscopy of SMGs. However, to date the sensitivity of mm-wave facilities has limited the approach to followup of bright, gravitationally lensed SMGs (e.g. Weiss et al. 2009; Swinbank et al. 2010; Harris et al. 2012; Vieira et al. 2013; Zavala et al. 2015).

While the IRAM Plateau de Bure Interferometer (PdBI) is sensitive enough to detect ^{12}CO in unlensed SMGs (e.g. Bothwell et al. 2013), its 3.6 GHz bandwidth receivers limit this approach due to the large time requirement for blind searches of ^{12}CO lines in redshift space via multiple frequency tunings. Walter et al. (2012) observed the *Hubble Deep Field*-North (HDF-N) field with the PdBI over the full 3 mm window to a similar depth as the Bothwell et al. (2013) survey, requiring 110 h on-source. In addition to blindly detecting two faint ^{12}CO emitting galaxies, they identified the redshift of the $S_{850\,\mu m} \sim 5$ mJy HDF850.1 as $z = 5.3$. The 8-GHz instantaneous, dual-polarization bandwidth of ALMA, coupled with its sensitivity, improves this approach, but still makes it a relatively expensive prospect to blindly obtain ^{12}CO redshifts for even the brightest SMGs with $S_{850\,\mu m} \sim 8$ mJy.

In this paper, we describe a photometric redshift guided, mm-wave search for ^{12}CO line emission from HS1700.850.1, one of the brightest unlensed SMGs ever discovered, with $S_{850\mu m} = 19.1$ mJy. The target field was chosen from the 24 survey fields of the Keck Baryonic Structure Survey (KBSS – e.g. Rudie et al. 2012). Several of these fields show strong galaxy overdensities (e.g. Steidel et al. 2000, 2005, 2010), and together represent a complete, unbiased census of overdensities in a well-calibrated field galaxy survey at $z > 2$. The HS1700+64 field, in which HS1700.850.1 was found, hosts a well-characterized $z = 2.30$ protocluster, studied in detail in several works (Shapley et al. 2005; Steidel et al. 2005; Digby-North et al. 2010). The faintness of HS1700.850.1 at near-IR/optical wavelengths precluded spectroscopic observations, despite lying in this well-studied field.

We use cosmological parameters $\Omega_m = 0.3$, $\Lambda = 0.7$, and $H = 70$ km s^{-1} Mpc^{-1} throughout the paper; at $z = 2.82$, this corresponds to an angular scale of 7.94 kpc arcsec^{-1}, or 0.48 Mpc arcmin^{-1}.

2 OBSERVATIONS AND STRATEGY

The HS1700+64 field was targeted with Submillimetre Common-user Bolometer Array-2 (SCUBA-2) at the James Clerk Maxwell Telescope (JCMT) as part of a sub-mm-wave followup of six KBSS fields (Lacaille et al., in preparation), covering ∼0.19 deg^2. The brightest source in this 850 μm survey is HS1700.850.1 with $S_{850\,\mu m} = 19.1 \pm 0.8$ mJy. Fig. 1 shows cutouts of HS1700.850.1 at SCUBA-2 and *Spitzer* wavelengths, revealing a likely identification at 4.5 μm.

The HS1700+64 field contains a massive proto-cluster at $z = 2.30$ (Steidel et al. 2005), and given its 1.5 arcmin proximity to the cluster centre, HS1700.850.1 was considered a likely cluster member. HS1700.850.1 has two candidate *Spitzer*-IRAC identifications within 4 arcsec of the 850 μm centroid, one of which is associated with a well-detected complex of $z = 2.305$ galaxies. IRAM-PdBI observations targeting ^{12}CO(3–2) and [CI] at $z = 2.305$ in the 3 and 2 mm bands, respectively, showed no detectable line emission, indicating this redshift was incorrect (Fig. 2). However, the WIDEX receiver's 3.6 GHz wide spectrum revealed a strong line detected serendipitously at 150.6 GHz near the edge of the chosen 2-mm-band setting (Figs 2 and 3). Two followup observations targeted the three most likely redshifts, assuming this 150.6 GHz line was a ^{12}CO rotational transition, as described in Section 3.1. We also draw on *Spitzer*-infra-red array camera (IRAC), ground-based and *HST* optical data sets described by Steidel et al. (2011). All flux measurements are shown in Fig. 4, and discussed in Section 3.1.

2.1 JCMT/SCUBA-2 observations

SCUBA-2 observations were conducted in Band 2 weather conditions ($\tau_{225\,GHz} < 0.08$) over six nights between May 23 and 2013 Oct.

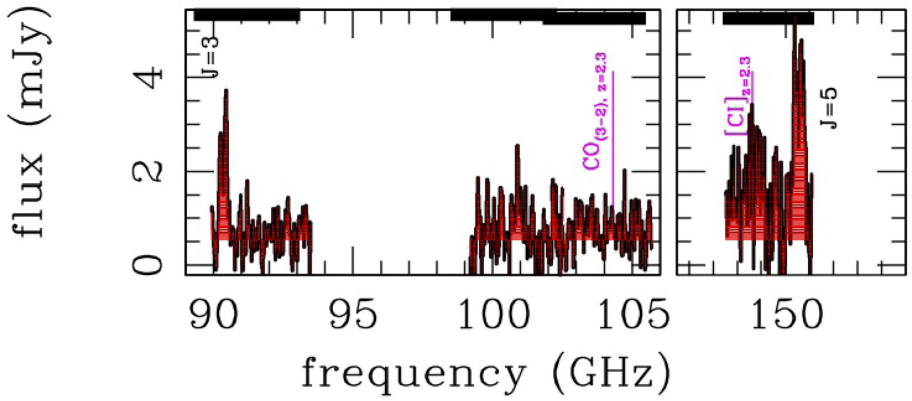

Figure 2. A composite of all spectral scans towards HS1700.850.1, shown at a velocity resolution of 60 km s^{-1} (arbitrary flux scaling). ^{12}CO emission lines are seen at ∼90.2 and 150.6 GHz, the latter corresponding to ^{12}CO(5–4). The originally targeted $z = 2.31$ ^{12}CO and [CI] line frequencies are highlighted (magenta), with a curious excess seen at the [CI] frequency. The four tuning bands are marked with heavy lines, showing a slight overlap near 101 GHz.

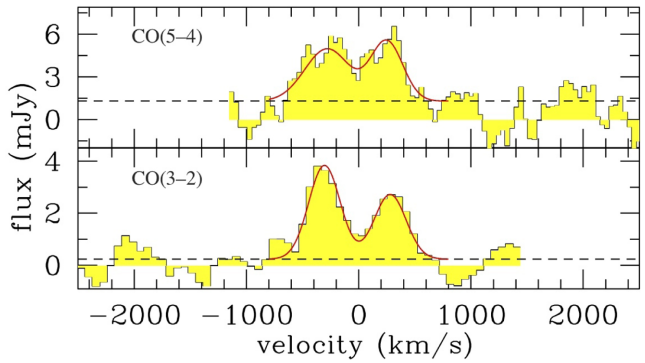

Figure 3. Spectra of the ^{12}CO(3–2) and ^{12}CO(5–4) lines towards HS1700.850.1. The spectral resolution is 60 km s^{-1} for both lines. We find only marginal evidence for any spatial separation in the two peaks of the CO lines <1 arcsec. Double Gaussian fits to each line profile are overlaid, emphasizing the ∼50 per cent higher peak flux in the blue component of the CO(3–2) profile. Line ratio and dynamical modelling issues are discussed in detail in the text.

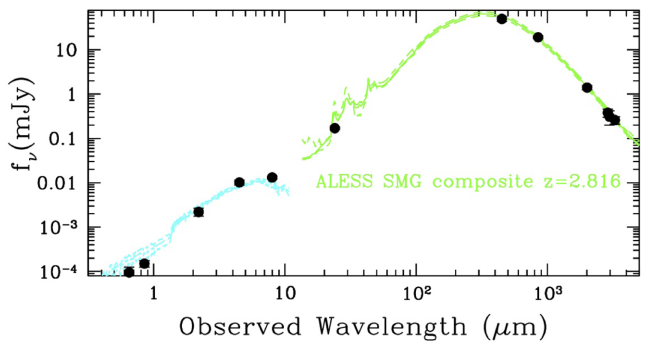

Figure 4. The SED of HS1700.850.1, with the Swinbank et al. (2014) composite SMG template overlaid. Significantly hotter or cooler SEDs than this ∼35 K template are reasonably rejected by the photometry. The template is split at a rest frame 10 μm in order to fit the optical/near-IR faint component as decoupled from the luminous far-IR to sub-mm dust component. The far-IR luminosity of this model is 3.8×10^{13} L$_\odot$.

15, totalling 15 h of on-sky integration in individual 30 min scans. A standard 3 arcmin diameter 'daisy' mapping pattern was used, which keeps the pointing centre on one of the four SCUBA-2 sub-arrays at all times during exposure. Data reduction followed standard recipes (e.g. Geach et al. 2013), with individual 30 min scans reduced using the dynamic iterative map-maker of the SMURF package (Jenness et al. 2011), flat-fielding, and then solving for model components assumed to make up the bolometer signals (atmospheric, astronomical, and noise terms). The signal from each bolometer's time stream is then re-gridded on to a map, with the contribution to a given pixel weighted according to its time-domain variance. Filtering of the time series is performed in the frequency domain, with band-pass filters equivalent to angular scales of $2 < \theta < 120$ arcsec, along with 10σ deviation *spike* removal in a moving boxcar, and DC step corrections. Finally, since we are interested in (generally faint) extragalactic point sources, we apply a beam matched filter to improve point source detectability, resulting in a map that is convolved with an estimate of the 850 μm beam. The map reaches central noise levels of $\sigma_{850} = 0.51$ mJy and $\sigma_{450} = 6.4$ mJy.

2.2 IRAM/PdBI observations

The IRAM-PdBI observations were taken in D configuration using the five-antenna sub-array (properties of the observing runs and resulting synthesized beam sizes are summarized in Table 1), at a pointing centre: RA = 17 01 17.779, Dec. = +64 14 37.85, J2000.0, taken from the SCUBA-2 centroid. Flux calibration was achieved by observing various calibrators (3C273, 3C345, B0234+285, B1749+096). The quasar B1300+580 was used as a phase and amplitude calibrator. Data were processed using the most recent version of the GILDAS software. We resampled the cubes in 90 km s^{-1} channels, and imaged them using the GILDAS suite *mapping*, adopting natural weighting. The full PdBI spectrum is shown in Fig. 2. To obtain flux measurements, we deconvolved the visibilities using the CLEAN task with natural weighting, and applied the corresponding primary beam correction (negligible at the small 3 arcsec offset of the HS1700.850.1 position).

2.3 SMA observations

Followup Sub-Millimetre Array (SMA) observations were performed on 2014 August 15 and September 7 in the compact and extended configurations, respectively (beam sizes ∼2 and ∼0.85 arcsec, respectively) in good weather ($\tau_{225\,\mathrm{GHz}} \sim 0.08$) with a total on-source integration time of approximately 6 h. The USB was tuned to 345 GHz, and combined with the LSB for an effective bandwidth of ∼4 GHz at 340 GHz, which yielded a final rms of

Table 1. PdBI observations log.

Run-ID	Centre freq (GHz)	$t_{\rm int}^{a}$ (h)	Depth^{b} (mJy)	Obs date	Beamsize (arcsec^2)
S14ck001	103.8	3.34	0.60	09/06/14	5.1 × 4.2
S14ck002	149.2	3.45	1.12	11/06/14	3.5 × 2.7
D14d001	100.8	1.50	0.95	28/07/14	4.7 × 4.0
D14d002	91.7	3.15	0.43	04/08/14	4.8 × 4.1

Notes. [a]Five-antenna integration.
[b]Per 50 MHz channel.

1.1 mJy. The pointing centre was the same as that for the PdBI observations described above. The data were calibrated using the MIR software package (Scoville et al. 1993), modified for the SMA. Passband calibration was done using 3C 84, 3C 111, and Callisto. The absolute flux scale was set using observations of Callisto and is estimated to be accurate to better than 20 per cent. Time-dependent complex gain calibration was done using 1858+655 (0.6 Jy, 21°.8 away) and 1827+390 (1.8 Jy, 37°.7 away). We detect HS1700.850.1 in the synthesized image at $\sim 13\sigma$. The calibrated visibilities were best fitted by a single point source with an integrated flux density of $S_{890\,\mu\rm m} = 14.5 \pm 1.1$ mJy at a position of α(J2000) = 17 01 17.779 and δ(J2000) = +64 14 37.85, consistent within 0.3 arcsec with the centroid of the line and continuum measurements from PdBI. The astrometric uncertainties are $\Delta\alpha = 0.24$ arcsec (0.20 arcsec systematic; 0.13 arcsec statistical) and $\Delta\delta = 0.22$ arcsec (0.19 arcsec systematic; 0.10 arcsec statistical).

3 RESULTS

3.1 The redshift search

Our original IRAM-PdBI observations searched for the ^{12}CO and [CI] lines in HS1700.850.1 at a redshift ∼2.30. This was motivated by it lying near the core of a massive $z = 2.31$ protocluster in the KBSS (Steidel et al. 2011), and having a plausible 4.5 μm identification with a complex of known $z = 2.305$ BX galaxies. Being such an extreme source we would not expect to find it by chance in the small 0.03 deg^2 H1700+64 pointing, or even in the 0.19 deg^2 survey of the six KBSS fields without the high-density environment of the proto-cluster in this field. Using typical single-dish 850 μm counts (Coppin et al. 2006; Weiss et al. 2009) we expect a surface density of just 0.01 deg^{-2} for such 19 mJy sources. The source counts of the brightest sub-mm sources (S870 μ m > 9 mJy) measured by ALMA fall more steeply than those measured with lower resolution single-dish observations due to the multiplicity of the brightest sources when observed at arcsec resolutions (e.g. Karim et al. 2013). As HS1700.850.1 retains at least ∼15 mJy in the interferometric followup (and as much as 19 mJy if the compact configuration SMA data are taken at face value), the expected >15 mJy source density drops by another factor of 10 based on the ALMA-derived count of Karim et al. (2013) or Simpson et al. (2015b).

The IRAM-PdBI observations showed no such lines at the expected frequencies, and thereby implied that the proposed identification and redshift of $z \sim 2.31$ was incorrect. As the 7.2 GHz of frequency coverage did reveal a strong line detected serendipitously at 150.6 GHz near the edge of the 2 mm setting, we began a search to identify the correct redshift. The centroid of this 150.6 GHz line detection, as well as the PdBI 2 and 3 mm continuum detections of HS1700.850.1, localizes the emission from the source within optical/IR imagery to within ∼0.5 arcsec (Fig. 1), while followup SMA

Table 2. Photometry of HS1700.850.1.

Band	Flux	Instrument
91.7 GHz	0.25 ± 0.07 (mJy)	PdBI
100.8 GHz	0.31 ± 0.13 (mJy)	PdBI
103.8 GHz	0.38 ± 0.08 (mJy)	PdBI
149.2 GHz	1.39 ± 0.15 (mJy)	PdBI
850 μm	19.1 ± 0.8 (mJy)	SCUBA-2
870 μm	14.5 ± 1.1 (mJy)	SMA
450 μm	45 ± 6 (mJy)	SCUBA-2
24 μm	171 ± 7 (μJy)	MIPS
8.0 μm	13.2 ± 1.2 (μJy)	IRAC
4.5 μm IRAC	10.2 ± 0.9 (μJy)	IRAC
K_s(2.18 μm)	23.20 ± 0.13 (AB mag)	P200/WIRC
J(1.25 μm)	24.4 ± 0.2 (AB mag)	P200/WIRC
I(F814W)	25.8 ± 0.2 (AB mag)	*HST*/ACS
$\mathcal{R}$ [a]	26.1 ± 0.3 (AB mag)	WHT/PFC
g'	27.0 ± 0.3 (AB mag)	WHT/PFC
u'	>27.1, 3σ (AB mag)	WHT/PFC

Note. [a] The $\mathcal{R}$ filter is centred at 6900 Å and thus redder than the standard R – close to mid-way between SDSS r' and i' in effective wavelength.

870 μm continuum imaging unequivocally associates the 850 μm SCUBA-2 source to a single IRAC galaxy which is well detected in the *HST* F814W image (Fig. 1) revealing a faint disturbed, tadpole-like galaxy. Ground-based imagery marginally detects the galaxy at $\mathcal{R} = 26.1$, $g = 27$, $U > 27.1$, making optical spectroscopy very difficult, and the $z = 2.82$ redshift would be difficult for near-IR spectroscopy, although the $K_{s,\,\rm AB} = 23.2$ is feasible in general with a 10 m telescope. Note that these colours (e.g. $g' - \mathcal{R} = 0.9$ mag) make sense for a heavily reddened object at $z = 2.82$. However, the detection at g' band places loose constraints on the redshift to $z < 4$, while the comparable IRAC fluxes, $S(4.5\,\mu\rm m) = 10.2$ μJy and $S(8.0\,\mu\rm m) = 13.2$ μJy, suggest the 1.6 μm stellar bump should lie between, ranging between $2.4 < z < 3.7$. The very red $K_s - 4.5$ μm colour (1.8 mag AB) is large, though consistent with a high stellar mass object. The MIPS 24 μm flux of 0.17 mJy compared to the $S_{850\,\mu\rm m}$ flux suggests that PAH emission is not contributing to the 24 μm band, pushing the redshift to $z > 2.5$, as illustrated in the SED template fit (Fig. 4). Our final constraint on the redshift comes from the long-wavelength photometry (Fig. 4 and Table 2), where 3 mm, 2 mm, 870 μm, and 450 μm fluxes suggest a similar range of $2.5 < z < 4.5$ for a likely range of SMG dust temperatures, $25 < T_{\rm d} < 45$ K.

While these constraints may not seem very useful, the fact that we have a solid line detection at 150.6 GHz means that only three possible ^{12}CO identifications provide redshifts in this range: ^{12}CO(4–3) at $z = 2.82$, ^{12}CO(5–4) at $z = 3.58$, or ^{12}CO(6–5) at $z = 4.37$. Aided by these photometric redshift estimates, in two subsequent PdBI followup observations we searched for $z = 3.58$ ^{12}CO(4–3) at 100.4 GHz, and then at 91.5 GHz searched simultaneously for

$z = 2.82$ ^{12}CO(4–3) and [CI] at $z = 4.37$. With a detection of a second line (Fig. 2) we confirmed the redshift $z = 2.816$ for one of the most intrinsically luminous galaxies in the distant Universe ($L_{\rm FIR} \sim 5 \times 10^{13} {\rm L}_{\odot}$, Section 3.3) and secured a second ^{12}CO line for astrophysical diagnostics. Blind ^{12}CO redshifts for unlensed SMGs are still exceedingly rare in the literature. We are only aware of Daddi et al. (2009) GN20 at $z = 4.05$ (a truly serendipitous discovery), and the $z = 5.2$ for HDF850.1 (Walter et al. 2012).

3.2 Source properties

HS1700.850.1 is very bright at 850 μm, but shows no sign of lensing – the nearest galaxy detected is the low-mass star-forming galaxy BX951 2.9 arcsec away ($z = 2.3053$, $M^* = 2 \times 10^9$ M$_{\odot}$). HS1700.850.1 is thus not suffering from differential lensing and associated modelling issues and biases that could affect our interpretation of the ^{12}CO lines. The ^{12}CO spectra are shown zoomed in at a velocity resolution of 60 km s^{-1} in Fig. 3. Both lines are detected at high significance [11.3 σ and 6.9 σ for continuum subtracted (3–2) and (5–4) lines, respectively, in integrated intensity]. The line profiles for both lines are similar and well described by a double Gaussian with a peak separations of 585 and 530 km s^{-1}for (3–2) and (5–4) ^{12}CO lines, respectively, and individual peak FWHMs of ∼330–470 km s^{-1}. While the (3–2) line shows an apparent peak flux asymmetry compared with the (5–4) peaks, in fact the flux ratios of the blue and red lines are quite similar, $r_{53,\,\rm blue} = 0.69 \pm 0.12$ and $r_{53,\rm red} = 0.59 \pm 0.09$. The parameters derived from Gaussian fits to both line profiles are given in Table 3. We find only marginal evidence for any spatial separation in the two peaks of either of the ^{12}CO lines <1 arcsec. The frequencies unambiguously identify the lines as CO(3–2) and CO(5–4). Combining the centroids of both lines, we derive a variance-weighted mean redshift for HS1700.850.1 of $z = 2.816 \pm 0.001$. While the observed frequencies might also be interpreted as ^{12}CO(6–5) and ^{12}CO(10–9) at $z = 6.64$, the ^{12}CO ladder is not equidistant in frequency which results in small differences for the frequency separation of the line-pairs as a function of rotational quantum number. The frequency separation is 58.58 and 58.53 GHz for the ^{12}CO line-pairs at redshifts 2.82 and 6.64, respectively. Our observations yield $\delta\nu = 58.58 \pm 0.02$ GHz, clearly consistent with the former, and supported by the photometric redshift.

With the precise redshift and the observed ^{12}CO line luminosities in hand, we can estimate the molecular gas content of HS1700.850.1. The observed global ^{12}CO(5–4) to ^{12}CO(3–2) line ratio (0.67 ± 0.09) implies that the CO emission is subthermally excited, at least for the CO(5–4) line. The average line ratio reported by Bothwell et al. (2013) for a sub-sample of their 30 SMGs is $r_{53} = 0.62$. This line ratio is similar to that observed for SMM J16359+6612 (Weiss et al. 2005) and we use a similar scaling to estimate a ^{12}CO(1–0) line luminosity of $L' \approx 1.86 \times 10^{11}$ K km s^{-1} pc^2. This translates into a molecular gas mass of $M_{\rm H_2} \approx 2.1 \times 10^{11}$ M$_{\odot}$ using a standard ULIRG conversion factor of 1.0 M$_{\odot}$ (K km s^{-1} pc^2)$^{-1}$ found for typical $z \sim 2.5$ SMGs in Bothwell et al. (2013), and including a 15 per cent contribution from helium [Downes & Solomon 1998 adopted 0.8 M$_{\odot}$ (K km s^{-1} pc^2)$^{-1}$.]

Table 3. Gaussian decomposition of the CO line spectra. Values for the total line are estimated from integrating the continuum-subtracted spectra, while the red and blue component properties are estimated from the Gaussian fits. Errors in redshift estimation are d$z = 0.001$. The measured FWHM for the total line is quoted as σ, 2.355× smaller. L'CO is in units of 10^{10} K km s^{-1} pc^2. Note that for α(CO) = 1 M$_{\odot}$ (K km s^{-1} pc^2)$^{-1}$, as estimated in Bothwell et al. (2013), $L'{\rm CO}_{1\text{-}0}$ = M(gas), which should then be corrected by an additional 15 per cent for helium.

	Blue	Red	Total
$z_{(3\text{-}2)}$	2.812	2.820	2.816
δv(3–2) [km s^{-1}]^a	− 305 ± 9	+280 ± 11	0
δv(5–4) [km s^{-1}]^a	− 280 ± 21	+250 ± 19	0
σ(3–2) [km s^{-1}]	140 ± 25	142 ± 20	400 ± 57^c
σ(5–4) [km s^{-1}]	200 ± 45	143 ± 24	349 ± 45^c
$I_{3\text{-}2}$ [Jy km s^{-1}]	1.26 ± 0.16	0.88 ± 0.13	2.32 ± 0.21
$I_{5\text{-}4}$ [Jy km s^{-1}]	1.84 ± 0.23	1.5 ± 0.21	3.44 ± 0.30
$L'{\rm CO}_{3\text{-}2}$	5.18	3.62	9.65
$L'{\rm CO}_{5\text{-}4}$	2.72	2.21	5.08
$L'{\rm CO}_{1\text{-}0}$ ^{b}	9.95	6.95	18.56

Notes. ^{a}Centre velocity relative to $z = 2.816$.
^{b}Derived using average $r_{31} = 0.32$ scaling relation of Bothwell et al. (2013).
^{c}These are the best-fitting single Gaussian to the entire line profile.

3.3 SED modelling

The SED of HS1700.850.1, with the Swinbank et al. (2014) composite SMG template overlaid, is shown in Fig. 4. Significantly hotter or cooler SEDs than this ∼35 K template are reasonably rejected by the photometry. The template is split at a rest frame 10 μm in order to fit the optical/near-IR faint component as decoupled from the luminous far-IR to sub-mm dust component. The far-IR luminosity of this model is 3.8×10^{13} L$_{\odot}$, translating to a SFR of 2500 M$_{\odot}$ yr^{-1} (Kennicutt 1983). HS1700.850.1 is not unusually faint in optical/IR magnitudes for SMGs with $S_{850\,\mu\rm m} \sim 3$–5 mJy, but its far-IR output is significantly higher, and it is thus proportionally far more obscured than ALESS SMGs (see Swinbank et al. 2014).

A hyper-z fit to the IRAC and near-IR photometry yields a stellar mass of 3×10^{11} M$_{\odot}$, assuming a Chabrier IMF. Together with the above gas mass estimate, the gas fraction is ∼40 per cent, and precludes using substantially higher conversion factors, $\alpha({\rm CO}) \gg 1$, which would drive the gas fraction up towards 100 per cent.

3.4 SMA and PdBI continuum maps and source multiplicity

The PdBI observations reveal only a single significant detection in both continuum and line emission, showing that there is no obvious multiplicity at 2 mm/3 mm or in CO lines. As such there are no nearby (<25 arcsec primary beam) ^{12}CO-luminous companions to HS1700.850.1. Similarly the SMA image does not detect any additional significant sources. The combined 3 mm continuum map reaches 0.35 mJy rms. At this depth we are sensitive to SMGs with SFRs ∼1000 M$_{\odot}$ yr^{-1}. The 2 mm continuum map reaches 1.2 mJy rms and should detect similar SFRs for a typical $\beta \sim 1.5$ dust SED. The SMA 870 μm map rms of 1.1 mJy is much more sensitive to dusty sources, and should detect galaxies with SFRs ∼ 300 M$_{\odot}$ yr^{-1}. We note that a CO-luminous DRG in this field with SFRs ∼ 200 M$_{\odot}$ yr^{-1} from Chapman et al. (2015) is not detected in any of these continuum maps, nor are any of the other known galaxies lying within the primary beam.

By considering only the SMA compact configuration data (2 arcsec beam size), we measure a larger flux density of 19.3 ± 2.8 mJy, close to that measured by SCUBA-2 in the 14.5 arcsec beam, although the large measurement error agrees with the extended configuration flux measurement within ∼2σ. Nonetheless, this may suggest there is either a modest conflict in the flux scale between

compact and extended configurations, or that the source may be marginally resolved on scales greater than the average beam size achieved in our extended configuration data, >0.85 arcsec. However, this is unusual for bright SMGs (Simpson et al. 2015a) which typically are resolved with ∼0.3–0.4 source sizes. Ubiquitous SMG multiplicity results from surveys (e.g. Wang et al. 2010; Hodge et al. 2013; Simpson et al. 2015b) and theoretical arguments (e.g. Hayward et al. 2012, 2013) would argue that there may well be faint companions within the SCUBA-2 beam, and the similarity of the compact SMA data flux may just be a lucky coincidence.

4 DISCUSSION

4.1 Gas dynamics

At first glance the double-peaked line profile suggests a circumnuclear molecular toroid. However, if such a stable molecular gas distribution would supply the large star formation rate (≈2500 $M_\odot$ yr^{-1}), we would expect a high gas excitation. The observed line ratio $r_{53} = 0.67 \pm 0.09$ is low compared to well-studied nearby starburst galaxies NGC 253 and M 82, although it is typical of that measured by Bothwell et al. (2013), a brightness temperature ratio $r_{53} = 0.62$, for SMGs with characteristic $L_{850\,\mu m}$ lower than HS1700.850.1 by a factors of 3× on average. However, the two line peaks could also be two disc components merging, individually unresolved. The line integrated gas properties between the spectral components are similar in the red and blue component line ratios ($r_{53,\,red} = 0.6 \pm 0.1$, $r_{53,\,blue} = 0.7 \pm 0.2$), contrasting the component line widths and central velocities which do differ between the different excitation lines. This argues that the (5–4) line may be coming from a different volume of gas than the (3–2) line, which could be true in either a disc-like or merger configuration. If the SMA dust continuum size is the same as the CO gas (<0.85 arcsec or <6.7 kpc), then either the disc or the merger is in a very compact state. We note that a ring-like rotating disc distribution of gas was strongly endorsed as an explanation for another similar double-peaked SMG, SMM J02399−0136 (Genzel et al. 2003), however from multi-frequency, high-resolution line mapping observations, Ivison et al. (2010) showed that the system comprises a multiple merger.

HS1700.850.1 is clearly a very massive system, and is in particular a very massive *baryonic* system. Observational studies of local ellipticals (Keeton 2001; Boriello, Salucci & Danese 2003; cf. Loewenstein & Mushotzky 2003) suggest that typically ∼30 per cent of the total mass within the optical effective radius will be dark; the interior regions of massive local disc galaxies have similarly low dark matter fractions (Combes 2002). By analogy with these local systems, HS1700.850.1 should have a baryonic mass of $\geq 4 \times 10^{11}\,\sin^{-2} i^{-1}$ $M_\odot$ within 7 kpc; $M_{gas} \sim 2 \times 10^{11}$ $M_\odot$ then implies that a limit to the stellar mass within the same radius is $\sim 2 \times 10^{11}$ $M_\odot$. The Kennicutt (1983) stellar initial mass function (IMF) models of Cole et al. (2001) imply that $M^* \sim 7 \times 10^{10}$ $M_\odot$ for the galaxy stellar mass function in the local Universe. Based on the stellar content of its inner 7 kpc, then HS1700.850.1 is already at least a $3M^*$ system, on its way to becoming a $\geq 4M^*$ system as it turns the remainder of its molecular gas into stars.

4.2 An Eddington-limited starburst?

If we assume that HS1700.850.1 is starburst dominated and make assumptions about the morphology and kinematics, we find it may be radiating close to or at the Eddington limit of its starburst. Elmegreen (1999) demonstrated that feedback from ongoing star formation sets a physical limit on the minimum size of a star-forming region. Radiation pressure from high-luminosity star formation regions should produce strong momentum-driven winds due to high dust opacity seen by the ultraviolet light produced by young stars (e.g. Netzer & Elitzer 1993). These winds are confined by the gravitational potential, which scales as $\Phi \sim f_g \sigma^2 \log D$ for an isothermal sphere (with the gas fraction f_g, stellar velocity dispersion σ, diameter of the starburst region D). In the optically thin limit (appropriate for optically thick clouds with a small volume filling factor embedded in the diffuse interstellar medium) and assuming a Chabrier (2003) IMF, this leads to a maximum star formation rate

$$\mathrm{SFR_{max}} = 360\,\sigma_{400}^2 D_{\rm kpc} \kappa_{100}^{-1}\ M_\odot\ \mathrm{yr}^{-1}. \quad (1)$$

We measure the scale size of the starburst $D_{\rm kpc}$ as the Gaussian FWHM of the SMA detected source, and σ_{400} as the line-of-sight ^{12}CO gas velocity dispersion in units of 400 km s^{-1} which is the best-fitting single Gaussian to the entire CO(3–2) line; κ_{100} is the dust opacity in units of 100 cm^2 g^{-1}, which we set to 1, but note that many dust models allow for significantly higher opacity, and in particular for the ultraviolet radiation produced by young massive stars during a starburst (e.g. Li 2001). HS1700.850.1 has a very high far-IR luminosity, with $L_{\rm FIR} \approx 4 \times 10^{13}$ $L_\odot$ and SFR ≈ 2500 $M_\odot$ yr^{-1} on a physical scale of <7 kpc. This very luminous SMG is therefore near the Eddington limit ≤2500 $M_\odot$ yr^{-1} for a starburst on those scales. The size/SFR ratio of HS1700.850.1 is typical of the more luminous SMG components identified with ALMA observations by Simpson et al. (2015a), suggesting near Eddington-limited starbursts are not unusual in the SMG population. This motivates obtaining additional higher resolution 870 μm and ^{12}CO observations of HS1700.850.1 to truly resolve the emission of this bright galaxy.

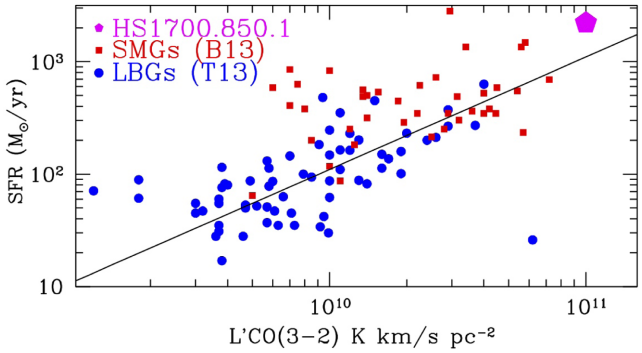

Figure 5. SFR versus L'CO(3–2) for various literature galaxies compared with HS1700.850.1 (normal star-forming galaxies – Tacconi et al. 2013; SMGs – Bothwell et al. 2013). CO(3–2) is adopted for maintaining all displayed galaxies as close to observed transitions as possible. We show L'(CO) for HS1700.850.1, revealing it is nominally under-luminous in ^{12}CO compared to other ultra-luminous *normal* star-forming galaxies, but not unusual compared to many SMGs in Bothwell et al. (2013) in lying a factor of 2–3× above the Tacconi et al. (2013) best-fitting relation.

4.3 $L'_{\rm CO}$ to $L_{\rm FIR}$ comparison with literature

We next turn to a discussion of HS1700.850.1 versus other ^{12}CO-detected sources, plotting $L'_{\rm CO}$-SFR for the known and published high-z sources (Fig. 5), and translating $L_{\rm FIR}$ to SFR in the SMG populations using standard conversions (Kennicutt 1983). Of note is that HS1700.850.1 has a significantly higher $L'_{\rm CO}$ than any of

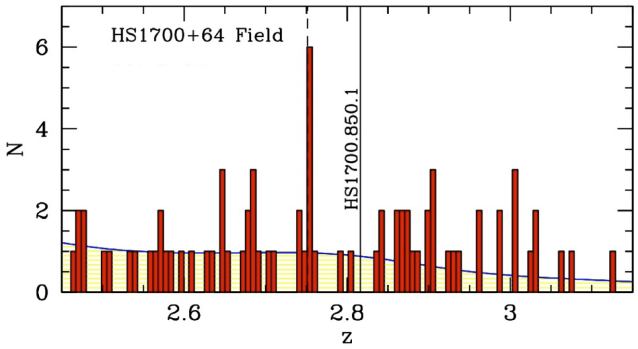

Figure 6. The environment of HS1700.850.1 derived from the LBG survey in the field, with 500 km s^{-1} bins to highlight any possible neighbouring galaxies (the closest one at $z = 2.807$ lies 5 arcmin away). HS1700.850.1 appears to reside in a relative void, although the selection function suggests only two expected LBGs in a 1500 km s^{-1} region for the 243 spectroscopic galaxies from $z = 1.5$–3.5 measured in this field (the overall redshift selection function for the continuum-selected redshift survey in all 15 fields of KBSS is shown as a blue line – see e.g. Steidel et al. 2014). There is a six-object galaxy spike at the redshift of the QSO HS1700+64 itself, contrasting the sparse environment of HS1700.850.1, while at $z = 2.31$ (off the plot axes) there is in fact a very large galaxy 'overdensity consistent with a forming proto-cluster (Steidel et al. 2005).

the 35 unlensed SMGs in the Bothwell et al. (2013) survey. Comparably ^{12}CO-luminous SMGs were found in a few cases – Ivison et al. (2013) identified a binary HyLIRG merger from a ∼200 deg^2 *Herschel* survey, while one lensed SMG from the ∼1300 deg^2 South Pole Telescope survey appears to be this luminous in ^{12}CO after a demagnification factor of ∼5 × (Hezaveh et al. 2013). Clearly finding SMGs with such high $L'_{\rm CO}$ has not been an easy task, even probing the widest field mm-wave surveys.

HS1700.850.1 is somewhat under-luminous in ^{12}CO for its SFR (or a high efficiency star former) compared to the average relation from Tacconi et al. (2013) for *normal* star-forming galaxies (shown in Fig. 5). However, compared to SMGs from Bothwell et al. (2013), HS1700.850.1 is not unusual in lying 2–3× above the relation, an observation that supports application of the ULIRG conversion rate from $L'_{\rm CO}$ to total molecular gas mass.

4.4 The environment of HS1700.850.1

Given the extreme nature of HS1700.850.1, we explore whether the surroundings of this SMG are unusually clustered. The environment of HS1700.850.1 is traced in great detail by the LBG survey in the field, presented in Fig. 6 as a histogram binned to 500 km s^{-1} to highlight any possible neighbouring galaxies. HS1700.850.1 appears to reside in a sparse region, with the closest (and only) neighbouring galaxy within ±1500 km s^{-1} at $z = 2.807$ and lying 5 arcmin (2.5 Mpc) away. The LBG selection function appropriate to this field (see Steidel et al. 2014) suggests that only two LBGs are expected in a 1500 km s^{-1} region from the 243 spectroscopic LBGs with measured redshifts in this field, thus finding only one about HS1700.850.1 is not statistically significant. There is one modest overdensity of six sources at $z = 2.751$, which includes the QSO HS1700+64 itself, contrasting with the sparse HS1700.850.1 environment nearby. Off the figure, at $z = 2.31$, there is a large overdensity consistent with a forming proto-cluster (Steidel et al. 2005).

Using the extensive spectroscopic data base of the KBSS survey, Trainor & Steidel (2012) study similar extreme sources to HS1700.850.1 at $z = 2.5$–3.5 – HyLIRG quasars (HLQSOs). They find the HLQSOs themselves are associated with a $\delta \sim 7$ overdensity in redshift when considered on scales of ∼5 h^{-1} Mpc, corresponding to a velocity scale of $\sigma_{\rm v,\,pec} = 200$ km s^{-1} and a projected scale of $R \sim 200$ proper kpc. By studying the redshifts of galaxies around each HLQSO, they find, however, that there are no overdense peaks of similar significance. Repeating this procedure on random galaxy redshifts shows that the HLQSOs are correlated with much more significant small-scale overdensities than the average galaxy. They deduce that each HLQSO in their sample inhabits a DM halo with mass $\log(M_{\rm h}/{\rm M}_\odot) > 12.1 \pm 0.5$, or a median halo mass of $\log(M_{\rm h,\,med}/{\rm M}_\odot) = 12.3 \pm 0.5$. Crucially, the number density of these haloes exceeds the number density of HLQSOs by a factor of ∼10^6–10^7, prompting the conclusion that the host haloes of HLQSOs are not rare. Clearly, HS1700.850.1 follows this trend, inhabiting an environment that is indistinguishable from the average field galaxy density in Fig. 6.

The scarcity of HLQSOs is likely due to an extremely improbable small-scale phenomenon that produces HLQSOs, possibly related to an atypical galaxy interaction geometry or similar scenario, or else extremely short durations of the events. Analogously in HS1700.850.1 and other extreme SMGs, an unlikely merger trajectory perhaps with unusually gas-rich progenitors (e.g. Narayanan et al. 2010) may explain rare bursts approaching $S_{850\,\mu{\rm m}} \sim 20$ mJy and $L_{\rm IR} \sim 2 \times 10^{13}$ L$_\odot$ (e.g. Ivison et al. 2013). This motivates obtaining more detailed followup of the resolved double-peaked ^{12}CO emission in HS1700.850.1 to better understand the circumstances generating such enormous star formation rates and illuminated dust masses. We might also hypothesize that a very short duration starburst could explain the extreme luminosity of HS1700.850.1. For example, if we assumed that every $S_{850\,\mu{\rm m}} = 15$–20 mJy SMG was a brief episode in the more numerous 5 mJy SMG population (1000× more numerous in the ALMA-based counts of Simpson et al. 2015b, but still very luminous starbursts in themselves), then the HyLIRG burst would last only 50 kyr of a characteristic burst of 50 Myr (e.g. Chapman et al. 2005; Tacconi, Neri & Chapman 2006). This may not be a well-motivated scenario – such a short time-scale could likely only be driven by intense, hot AGN activity, yet there is no sign of an AGN in HS1700.850.1. Further, an AGN could not boost the 850 μm emission while keeping the typical SMG appearance in Fig. 4. Most likely the SMG HyLIRGs are driven by a combination of factors.

Another estimate on the halo mass can be obtained using dynamical mass estimates from the peculiar velocities and the projected scale of the galaxy overdensities. With this approach Trainor & Steidel (2012) estimate HLQSOs are on average associated with even larger group-sized environments with total mass $\log(M_{\rm grp}/{\rm M}_\odot) \sim 13$. The SMG clustering analysis in Hickox et al. (2012) suggested that the SMG population is hosted by haloes of comparable mass (see also Blain et al. 2004). This overdense environment with small relative velocities would increase the probability of a rare event, but an unusual merger configuration is still likely required to generate such large luminosities. In HS1700.850.1, even a group environment of this mass is unlikely based on the lack of explicit companions within 1500 km s^{-1} and within ∼2.5 Mpc. However, an ∼10^{13} M$_\odot$ halo will typically only have a couple of bright LBG-class galaxies in it, and might be easy to miss in an incomplete spectroscopic survey.

The Trainor & Steidel (2012) analysis has clearly demonstrated that HyLIRG-class sources do not require environments very different from their much less luminous counterparts. Evidently, the exceedingly low space density of at least HLQSOs (∼10^{-9} Mpc^{-3})

results from a one-in-a-million event on scales ≪1Mpc, and not from being hosted by rare dark matter haloes. HS1700.850.1 appears to inhabit a similarly typical halo. A moderate mass environment was also noted for a highly significant association of eight SMGs at $z \sim 1.99$ by Chapman et al. (2009), whilst revealing that $z = 2$–3.5 SMGs generally do not align well with LBG overdensities within the GOODS-N survey field. Similar anti-biasing of SMGs is noted in the ECDFS field (Danielson, in preparation). Notable exceptions exist at higher redshifts, including a $z = 4.05$ galaxy overdensity found through an association of bright SMGs (Daddi et al. 2009), the COSMOS $z = 5.1$ structure (Capak et al. 2011), and HDF850.1, which apparently lies in a $z = 5.3$ galaxy overdensity (Walter et al. 2012).

Miller et al. (2015) used the Hayward et al. (2013) model for the SMG population to estimate typical environments of the brightest SMGs and associations of multiple SMGs found in ∼500 Mpc^3 volumes. This model is based on mock galaxy catalogues derived from the Bolshoi simulation (Klypin et al. 2001; Behroozi, Wechsler & Conroy 2013) and insights obtained from performing radiative transfer on hydrodynamical simulations (Hayward et al. 2011, 2013). Miller et al. (2015) find the SMGs inhabit a range of mass scales going down to the average cosmic density in the simulation, and rarely are found in the most massive regions at these $z = 2$–3 epochs (although at significantly higher redshifts they are better tracers of the most massive regions). The surrounding LBG survey indeed suggests HS1700.850.1 is statistically consistent with inhabiting the average cosmic density.

5 CONCLUSIONS

We presented an IRAM-PdBI spectral survey of the HyLIRG HS1700.850.1, the brightest 850 μm source found in the SCUBA-2 survey of the HS1700+64 field, and indeed all six SCUBA-2/KBSS fields. Our primary goal was to identify its redshift, guided by photometric redshift estimates in the optical through far-IR, and study its properties and environment. We conclude the following.

(i) The redshift for HS1700.850.1 is $z = 2.816$, secured through the ^{12}CO(3–2) and (5–4) lines, validating the use of crude photometric redshifts to guide ^{12}CO redshift searches.

(ii) The clear doubled-peaked profile of HS1700.850.1 in both CO transitions is likely a result of an end stage merger, within 7 kpc, as constrained by the size of the 850 μm emission.

(iii) HS1700.850.1 exhibits typical $L'_{\rm CO}$ for its far-IR luminosity or SFR compared to other unlensed SMGs, although its $L'_{\rm CO}$ is significantly larger than any SMGs identified in the Bothwell et al. (2013) survey, amongst the most luminous CO emitters known in the Universe – comparable to the HyLIRG merger found from 200 deg^2 in Ivison et al. (2013). The SFR and size constraints suggest HS1700.850.1 is emitting close to its Eddington limit.

(iv) The environment of HS1700.850.1 is indistinguishable from the average field galaxy density, and no nearby LBG companions are identified within 1500 km s^{-1}. The HyLIRG burst could result from a 10^{-6} unlikely event on scales ≪1Mpc, and not from being hosted by a rare dark matter halo, but could also be due to a very short ∼50 kyr burst time-scale.

ACKNOWLEDGEMENTS

We thank an anonymous referee for constructive comments on the manuscript. IRAM is supported by INSU/CNRS (France), MPG (Germany) and IGN (Spain). The submillimetre array (SMA) is a joint project between the Smithsonian Astrophysical Observatory and the Academia Sinica Institute of Astronomy and Astrophysics and is funded by the Smithsonian Institution and the Academia Sinica. We thank summer students K. Lacaille and R. Perry for their work on the KBSS-SCUBA2 survey project. SCC acknowledges NSERC and CFI for support. FB acknowledges support through the Collaborative Research Centre 956, sub-project A1, funded by the Deutsche Forschungsgemeinschaft (DFG). IRS acknowledges support from STFC, a Leverhulme Fellowship, the ERC Advanced Investigator programme DUSTYGAL 321334 and a Royal Society/Wolfson Merit Award. JEG acknowledges support from the Royal Society.

REFERENCES

Behroozi P. S., Wechsler R. H., Conroy C., 2013, ApJ, 770, 57
Bertoldi F. et al., 2007, ApJS, 172, 132
Blain A., Chapman S., Smail I., Ivison R., 2004, ApJ, 611, 725
Boriello A., Salucci P., Danese L., 2003, MNRAS, 341, 1109
Borys C., Chapman S., Halpern M., Scott D., 2003, MNRAS, 344, 385
Bothwell M. et al., 2013, MNRAS, 205, 1511
Capak P. L. et al., 2011, Nature, 470, 233
Chabrier G., 2003, PASP, 115, 763
Chapman S., Blain A., Smail I., Ivison R., 2003, Nature, 422, 695
Chapman S., Blain A., Smail I., Ivison R., 2005, ApJ, 622, 772
Chapman S., Blain A., Ibata R., Ivison R., Smail I., Morrison G., 2009, ApJ, 691, 560
Chapman S. et al., 2015, MNRAS, 449, L68
Cole S. et al., 2001, MNRAS, 326, 255
Combes F., 2002, New Astron. Rev., 46, 755
Coppin K. et al., 2006, MNRAS, 372, 1621
Daddi E., Dannerbauer H., Elbaz D., Dickinson M., Morrison G., Stern D., Ravindranath S., 2009, ApJ, 673, L21
Digby-North J.A. et al., 2010, MNRAS, 407, 846
Downes D., Solomon P. M., 1998, ApJ, 507, 615
Elmegreen B. G., 1999, ApJ, 517, 103
Fu H. et al., 2013, Nature, 498, 338
Geach J. et al., 2013, MNRAS, 432, 53
Genzel R., Baker A. J., Tacconi L. J., Lutz D., Cox P., Guilloteau S., Omont A., 2003, ApJ, 584, 633
Greve T. R., Ivison R. J., Bertoldi F., Stevens J. A., Dunlop J. S., Lutz D., Carilli C. L., 2004, MNRAS, 354, 779
Harris A. I. et al., 2012, ApJ, 752, 152
Hayward C. C., Keres D., Jonsson P., Narayanan D., Cox T. J., Hernquist L., 2011, ApJ, 743, 159
Hayward C. C., Jonsson P., Keres D., Magnelli B., Hernquist L., Cox T. J., 2012, MNRAS, 424, 951
Hayward C. C., Narayanan D., Keres D., Jonsson P., Hopkins P. F., Cox T. J., Hernquist L., 2013, MNRAS, 428, 2529
Hezaveh Y. et al., 2013, ApJ, 767, 132
Hickox R. C. et al., 2012, MNRAS, 421, 284
Hodge J. et al., 2013, ApJ, 768, 91
Ivison R. J., Smail I., Le Borgne J.-F., Blain A. W., Kneib J.-P., Bezecourt J., Kerr T. H., Davies J. K., 1998, MNRAS, 298, 583
Ivison R., Smail I., Papadopoulos P. P., Wold I., Richard J., Swinbank A. M., Kneib J.-P., Owen F. N., 2010, MNRAS, 404, 198
Ivison R. J., Papadopoulos P. P., Smail I., Greve T. R., Thomson A. P., Xilouris E. M., Chapman S. C., 2013, MNRAS, 412, 1913
Jenness T., Berry D., Chapin E., Economou F., Gibb A., Scott D., 2011, in Evans I. N., Accomazzi A., Mink D. J., Rots A. H., ASP Conf. Ser. Vol. 442, Astronomical Data Analysis Software and Systems XX. Astron. Soc. Pac., San Francisco, p., 281
Karim A. et al., 2013, MNRAS, 432, 2
Keeton C. R., 2001, ApJ, 561, 46
Kennicutt R. C., Jr., 1983, ApJ, 272, 54
Klypin A., Kravtsov A. V., Bullock J. S., Primack J. R., 2001, ApJ, 554, 903
Li Z.-Y., 2001, ApJ, 556, 813

Loewenstein M., Mushotzky R. F., 2003, Nuclear. Phys. B Proc. Suppl., 124, 91
Miller T., Hayward C., Chapman S., Berhoozi P., 2015, MNRAS, 452, 878
Mocanu L. M. et al., 2013, ApJ, 779, 61
Narayanan D., Hayward C. C., Cox T. J., Hernquist L., Jonsson P., Younger J. D., Groves B., 2010, MNRAS, 401, 1613
Netzer N., Elitzer M., 1993, ApJ, 410, 701
Oliver S. et al., 2010, A&A, 518, L21
Planck Collaboration XXVIII, et al., 2014, A&A, 571, 28
Pope A. et al., 2006, MNRAS, 370, 1185
Rudie G. et al., 2012, ApJ, 750, 67
Scott K. et al., 2008, MNRAS, 385, 2225
Scoville N. Z., Carlstrom J. E., Chandler C. J., Phillips J. A., Scott S. L., Tilanus R. P. J., Wang Z., 1993, PASP, 105, 1482
Shapley A. E., Steidel C. C., Erb D. K., Reddy N. A., Adelberger K. L., Pettini M., Barmby P., Huang J., 2005, ApJ, 626, 698
Simpson J. et al., 2014, ApJ, 788, 125
Simpson J. et al., 2015a, ApJ, 799, 81
Simpson J. et al., 2015b, ApJ, 807, 128
Smail I., Ivison R. J., Blain A. W., Kneib J.-P., 2002, MNRAS, 331, 495
Steidel C., Adelberger K., Shapley A. E., Pettini M., Dickinson M., Giavalisco M., 2000, ApJ, 532, 170
Steidel C. C., Adelberger K. L., Shapley A. E., Erb D. K., Reddy N. A., Pettini M., 2005, ApJ, 626, 44
Steidel C., Erb D. K., Shapley A. E., Pettini M., Reddy N., Bogosavljevic M., Rudie G. C., Rakic O., 2010, ApJ, 717, 289
Steidel C., Bogosavljevic M., Shapley A. E., Kollmeier J. A., Reddy N. A., Erb D. K., Pettini M., 2011, ApJ, 736, 60
Steidel C. C. et al., 2014, ApJ, 795, 165
Swinbank A. M. et al., 2010, Nature, 464, 733
Swinbank M. et al., 2014, MNRAS, 438, 1267
Tacconi L. J., Neri R., Chapman S., 2006, ApJ, 640, 228
Tacconi L. J. et al., 2013, ApJ, 768, 74
Trainor R. F., Steidel C.C., 2012, ApJ, 752, 39
Vieira J. et al., 2013, Nature, 495, 344
Walter F. et al., 2012, Nature, 486, 233
Wang W.-H., Cowie L. L., Barger A. J., Keenan R. C., Ting H.-C., 2010, ApJS, 187, 251
Wardlow J. et al., 2011, MNRAS, 415, 1479
Weiss A., Downes D., Walter F., Henkel C., 2005, A&A, 440, L45
Weiss A., Ivison R. J., Downes D., Walter F., Cirasuolo M., Menten K. M., 2009, ApJ, 705, L45
Younger J. et al., 2008, ApJ, 688, 59
Younger J. et al., 2010, MNRAS, 407, 1268
Zavala et al., 2015, MNRAS, 452, 1140

This paper has been typeset from a TEX/LATEX file prepared by the author.